

Technical Note N-1331

THE COANDA-EFFECT OIL-WATER SEPARATOR: A FEASIBILITY STUDY

BY

D. Pal



February 1974

Sponsored by

Director of Navy Laboratories

Approved for public release; distribution unlimited.

Civil Engineering Laboratory  
Naval Construction Battalion Center  
Port Hueneme, CA 93043

TA  
417  
.N3  
no. 1331



UNCLASSIFIED

SECURITY CLASSIFICATION OF THIS PAGE (When Data Entered)

REPORT DOCUMENTATION PAGE		READ INSTRUCTIONS BEFORE COMPLETING FORM
1. REPORT NUMBER TN-1331	2. GOVT ACCESSION NO.	3. RECIPIENT'S CATALOG NUMBER
4. TITLE (and Subtitle) The Coanda-Effect Oil-Water Separator: A Feasibility Study		5. TYPE OF REPORT & PERIOD COVERED Not final
7. AUTHOR(s) D. Pal		6. PERFORMING ORG. REPORT NUMBER
9. PERFORMING ORGANIZATION NAME AND ADDRESS CIVIL ENGINEERING LABORATORY Naval Construction Battalion Center Port Hueneme, California 93043		8. CONTRACT OR GRANT NUMBER(s)
11. CONTROLLING OFFICE NAME AND ADDRESS		10. PROGRAM ELEMENT, PROJECT, TASK AREA & WORK UNIT NUMBERS ZF61-512-001-058
14. MONITORING AGENCY NAME & ADDRESS (if different from Controlling Office) Director of Navy Laboratories Washington, D.C. 20376		12. REPORT DATE February 1974
		13. NUMBER OF PAGES 42
		15. SECURITY CLASS. (of this report) UNCLASSIFIED
		15a. DECLASSIFICATION/DOWNGRADING SCHEDULE
16. DISTRIBUTION STATEMENT (of this Report)  Approved for public release; distribution unlimited.		
17. DISTRIBUTION STATEMENT (of the abstract entered in Block 20, if different from Report)		
18. SUPPLEMENTARY NOTES		
19. KEY WORDS (Continue on reverse side if necessary and identify by block number) Oil-water separator      Gravitation Coanda effect              Coalescence Effluent                      Ultrafiltration Centrifugation              Laminar flow		
20. ABSTRACT (Continue on reverse side if necessary and identify by block number)  An experimental investigation which establishes the feasibility of using the Coanda-effect in developing an oil-water separator is described. Tests conducted on an experimental model with an oil-water mixture containing 6% oil showed that the oil content in the effluent can be reduced to less than 3%. A three-stage separator has produced effluent in the range of 1%. Conceptual designs of a practical separator are discussed. The space		

DD FORM 1 JAN 73 1473 EDITION OF 1 NOV 65 IS OBSOLETE

UNCLASSIFIED

SECURITY CLASSIFICATION OF THIS PAGE (When Data Entered)

MBL/WHOI



0 0301 0040229 3

UNCLASSIFIED

SECURITY CLASSIFICATION OF THIS PAGE(When Data Entered)

20. Continued.

requirement for a Coanda-effect separator when compared with typical parallel-plate type separators of the same capacity is considerably smaller. Analytical expressions useful in designing a Coanda-effect separator of a given size are also given.

UNCLASSIFIED

SECURITY CLASSIFICATION OF THIS PAGE(When Data Entered)

## INTRODUCTION

The Navy is faced with very strict regulations covering the discharge of oily wastes from its ships and shore facilities. Such wastes primarily originate from ship's bilges and ballast waters, oil spill recovery operations, fuel storage and transfer systems, and garage and maintenance activities. Technology and hardware are being developed to process such wastes so that effluent will meet EPA requirements.

Current methods of separating oil from oil-water mixtures are centrifugation, gravitation, coalescence and ultrafiltration [1,2]. Centrifugation is an accepted method for separating water-oil dispersions or emulsions [2]. Commercial equipment is available for a wide range of applications. Despite their effectiveness, the power requirement, cost and maintenance of such systems is relatively high. The gravitation method of separating oil from oily wastes relies upon differences in densities of the fluids being separated. Commercially available API and Heil type parallel separators are based upon the gravitation principle. Because of the laminar flow requirements for separation such systems are normally bulky. Coalescence has been used quite extensively for removing finely dispersed water droplets from fuels. The basic mechanism behind this separation technique is the formation of larger oil drops on the coalescing material. The resulting larger drops are separated by gravity. The method, however suffers from fouling of the coalescing element and requires frequent maintenance. Finally, ultrafiltration uses a filtering process to separate water from oil. This method, although very effective, suffers from fouling of the filter element. The system requires frequent cleaning.

A new method of separating free oil from oil-water mixtures [3] is under investigation at the Naval Civil Engineering Laboratory \* (NCEL). This technique uses the fluid dynamic phenomenon, called "wall attachment, or Coanda effect", named after its discoverer, Henry Coanda. This effect is seen, for example, when one's finger is held close to a thin stream of water issuing from a tap or when tea is poured from a badly designed teapot-spout.

A preliminary investigation was conducted to establish the feasibility of using the Coanda effect for separating two immiscible liquids. This report describes in detail the feasibility program.

\*On 1 January 1974 redesignated the Civil Engineering Laboratory (CEL) of the Naval Construction Battalion Center, Port Hueneme, California.

## THEORY

Consider a thin jet sheet, quasi-two-dimensional, flowing into an unbounded region. The jet gets deflected towards an adjacent wall. When such wall is relatively close to the jet axis, the jet gets attached to and flows along the wall enclosing a separation bubble as shown in Figure 1. As is evident, the jet undergoes considerable curving during its attachment thus generating a centrifugal force field on it. This results in a lower pressure within the separation bubble. The pressure  $p_B$  in the separation bubble as derived in Appendix A is given by

$$P_{\infty} - p_B = J/b_o \frac{3\theta}{\sigma(1/t_1^2 - 1)} \quad (1)$$

where

- $P_{\infty}$  = free stream pressure,
- $J$  = jet momentum per unit span of the nozzle,
- $b_o$  = nozzle width,
- $\theta$  = angular location of the reattachment point,
- $\sigma$  = jet spread parameter,
- $t_1 = \tanh [\sigma y_1 / (s_1 + s_o)]$
- $s_1$  = axial distance between the reattachment point and the nozzle,
- $y_1$  = half width of the jet at the reattachment point,
- $s_o = \sigma b_o / 3$  = distance of the nozzle exit from a hypothetical origin of the jet.

Using the theory discussed in Appendix A, dimensionless pressure  $(P_{\infty} - p_B) b_o / J$  was plotted against the plate offset  $D/b_o$  for values of 7.7, 10 and 12 for the jet spread parameter  $\sigma$ . Figure 2 shows the pressure difference between the separation bubble and the ambient as a function of  $D/b_o$ .

For a jet composed of a mixture of two fluids which do not mix such as oil and water, the lighter fluid flowing along the plate side of the jet seeks the separation bubble and gets trapped by it. If an outlet is provided at the center of the bubble, the accumulated oil can be tapped out while the water and rest of the oil flows out of the device. This is the principle of operation of the Coanda-effect oil-water separator.

## EXPERIMENTAL PROGRAM

A test program was designed to determine the feasibility of

using the wall-attachment effect in separating two liquids. Two experimental elements with different flow parameters were built and tested. The experiments were conducted in the Mechanical Systems Laboratory at NCEL using a mixture of regular tap water and hydraulic oil as the test fluid.

### The Wall Attachment Elements

Based upon the theory developed in Appendix A, two experimental elements, namely, Elements No. 1 and No. 2 were designed. The 12-inch-long attachment wall of each element has an offset of 4 inches. The nozzles on Elements No. 1 and No. 2 are 1/4 and 3/8 inches wide respectively. The depth of flow passages on both elements is 1/4 inch. Element No. 1 was designed to carry 0.8 gpm of water flow whereas Element No. 2 has a flow carrying capacity of 1.5 gpm. The jet flow parameters such as reattaching distance  $x_R$ , jet center line radius  $r$  and its half width  $y_0$  at the reattachment point were determined from Figures A-2 through A-5 given in Appendix A. The jet spread parameter,  $\sigma$ , for the above calculations was chosen to be 12. The dimensions of the elements are listed in Table 1.

Each element consisted of three major components: top and bottom cover plates, and the middle plate with the flow passages machined in it. For ease of fabrication and to facilitate flow visualization during tests, each component plate of the Elements was made of transparent plexi-glass sheet. Further, to extract the accumulated oil in the separation bubble, a 1/4 inch diameter outlet was provided in the top cover plate of each element. The general layout showing major dimensions of the elements is given in Figure 3. The elements were assembled by gluing the two cover plates to the middle plate.

### Feasibility Tests

The experiments were performed using the test setup shown in Figure 4. The adjustment of supply water flow is possible by hand controlled valves provided on the flow line. A mixture of red hydraulic oil (Appendix B) and water was used as the test-fluid. The mixture was formed by injecting the oil into water stream before it entered the element. To form a homogenous mixture, the oil was released at the center of and parallel to the water flow in the pipe. The oil to the mixing junction was supplied by a variable flow pump (see details in Appendix B). The element was immersed in water throughout the test series. The supply water flow was measured by a rotameter. The static pressure in the water line was measured by conventional pressure gauges. The use of red oil in the test mixture allowed flow visualization through the elements. The photographs of flow patterns were taken by mounting a camera directly above the elements.

The feasibility tests were conducted by running the oil

Table 1. Parameters of the Test Elements

Parameter	Element No. 1	Element No. 2
Nozzle width, $b_o$ , inches	1/4	3/8
Wall offset, D, inches	4.0	4.0
Attachment wall length, $\ell$ , inches	12.0	12.0
Radius, $D/b_o$	16.00	10.67
Flow passage depth, h, inches	1/4	1/4
Designed water flow, gpm	0.80	1.50
Velocity at the nozzle at designed flow, feet/second	4.10	5.13
Reynold's number* at the nozzle, at designed flow	7119.7	13354.7
Jet Momentum at the nozzle, J lbs/ft	0.6794	1.595
Predicted pressure, $p_B$ , within the separation bubble (from Figure 2) inches of $H_2O$	0.1978	0.3935
Predicted Attachment distance, $x_R$ (from Figure A-5) inches	6.6	7.2
Predicted Jet center-line radius, r (from Figure A-4) inches	7.75	9.0
Predicted half width of the jet, y (from Figure A-3) inches	0.251	0.345

\*Kinematic viscosity of water at 60 degrees F taken as  
 $1.2 \times 10^{-5}$  ft<sup>2</sup>/second.



water mixture containing 6 to 8% oil by volume through the elements. The optimum water flow rates were 0.8 gpm through Element No. 1 and 1.5 gpm through Element No. 2 respectively. The mixture jet reattachment distances from the corners were measured for both elements. They were found to be 7 inches for Element No. 1 and 7.5 inches for No. 2. These values are very close to the theoretically computed values listed in Table 1. The test results indicated that a portion of the oil in the mixture jet did accumulate in the separation bubble zone of the flow. A photograph of the flow pattern (Figure 5) through Element No. 2 at its optimum flow rate clearly shows the accumulation of oil in the separation bubble. This oil when extracted contained about 50% water. Consequently, improved designs for collecting oil transferred into the separation bubble were sought. One such design is that of providing a chamber at the top of the separation bubble. This chamber is connected to the separation bubble by means of holes in the top cover plate of the element, see Figure 6. Under optimum conditions, the oil captured by the separation bubble flows into the collecting chamber through the connecting holes. Next, the oil collected in the chamber is transferred by siphoning to an oil storage tank. Two different designs of the collecting chambers were tested. These are shown in Figures 7 and 8. Due to its shape and its greater depth, the collecting chamber design shown in Figure 8 is more efficient in collecting the oil. Tests conducted on the elements with modified design show that about 50% of the oil in the input flow can be extracted in this manner, whereas the remaining oil flows out with the attached water jet. Furthermore, the oil being extracted contained about 5% water. Thus, a separating device based upon this concept appears to be capable of gross separation only. However, tests on elements with modified designs must be conducted before deriving final conclusions about the degree of separation obtainable. A photograph of the flow pattern through the Element No. 1 taken at its optimum flow rate is included as Figure 9. The accumulation of oil in the collecting chamber is clearly visible in this record.

#### Tests On A Multi-Stage Element

It was realized during the feasibility tests on the single-stage elements that to make the Coanda-effect separator suitable for practical applications, staging is necessary. The number of stages for the separator, however, depends upon the type of oily wastes being handled together with the quality of effluent desired.

During the course of this study a three-stage test element was designed and built to evaluate the effect of staging. Figure 10 shows the sketch of the element's middle plate with flow passages cut in it. Each stage of the element has a 1/4 inch

wide nozzle. The depth of element's flow passage was kept at 1/4 inch. The mixture jet in each stage is directed by a curved wall conforming to the curvature of a reattaching jet issuing parallel to a flat plate with an offset of 4 inches. This boundary was determined from flow governing equations given in Appendix A. The element was designed to handle 0.8 gpm of water flow through each stage. Each stage was provided with oil collecting chambers located directly on its separation bubble zone. The oil outlet line on each oil chamber was provided with a hand controlled valve for outgoing oil flow adjustment.

The element was tested using the setup shown in Figure 4. The tests were conducted by varying the oil in the mixture from 6 to 8%. The test results indicate that each stage separated about 50% of the oil from its input flow. The effluent at the third stage outlet contained about 1% oil. The oil being extracted had about 3 to 5% water. Figure 11 shows the element undergoing tests. The flow pattern through the element is shown in Figure 12. The accumulation of oil in the collecting chambers and the separated oil flowing through the outflow lines are shown in the flow record.

## DISCUSSION

### Jet Velocity Distribution

As mentioned earlier, the mixture jet during its attachment, develops a centrifugal acceleration. It was assumed prior to conducting the tests that the lateral acceleration so induced would force most of the oil in the jet into the separation bubble zone of the flow. The observed flow patterns through the experimental models on the other hand revealed that the oil particles were distributed uniformly over the entire cross-section of the jet. This important observation can be explained from theoretical considerations discussed in Appendix A.

Consider the reattaching jet velocity profile described by Equation 2:

$$u(s,y) = \left[ \frac{3J\sigma}{4\rho(s+s_o)} \right]^{1/2} \text{Sech}^2 \frac{\sigma y}{s+s_o} \quad (2)$$

where the various symbols are defined in Appendix A. The width of a two-dimensional jet expanding into a similar fluid at any axial location can be derived easily from a linear relationship given in References 4 and 5. The half width,  $y_1$  of the jet is given by

$$y_1 = \left( \frac{s+s_o}{s_o} \right) b_o / 2 \quad (3)$$

It can be seen from Equation 2 that the jet velocity  $u(s,y)$  is maximum at its center-line and is

$$u_{\max} = \left[ \frac{3J\sigma}{4\rho(s+s_o)} \right]^{1/2} \quad (4)$$

Next, it can be deduced from Equations 2 and 3 that the jet velocity  $u(s,y)$  drops to 0.1814  $u_{\max}$  at a distance equal to the half width of the jet from its center line. The centrifugal acceleration distribution in the jet can be derived from Equation 2 and is given by

$$\ddot{u}(s,y) = \frac{3J\sigma}{4\rho(s+s_o)(r\pm y)} \operatorname{sech}^4 \frac{\sigma y}{s+s_o} \quad (5)$$

Again it is evident from Equation 4 that the centrifugal acceleration,  $\ddot{u}(s,y)$  is maximum at the jet center line and is

$$\ddot{u}_{\max} = \frac{3J\sigma}{4\rho(s+s_o)r} \quad (6)$$

The acceleration drops sharply to approximately 0.0327  $u_{\max}$  at the jet half-width points.

The typical velocity and acceleration for the reattaching jets are shown in Figure 13. Because of the nature of lateral acceleration on the jet, the oil particles are distributed over the entire cross-section. Such a distribution of centrifugal acceleration affects the separating capability of a separator with this configuration.

The mixture jet velocity and hence its centrifugal acceleration distribution can be improved by modified designs. One such design is shown in Figure 14. The device uses a splitter located at the nozzle center-line to divide the mixture jet into two sub-jets which flow along the curved walls as shown. The mixture jets flowing through the device will have velocity distribution as shown in the figure, i.e., from a maximum near the curved

walls monotonically decreasing to zero at the separation bubble center. Such a velocity distribution will induce a monotonically decreasing centrifugal acceleration on the jet with a maximum near the wall. This configuration will force most of the oil into the separation bubble. The effluent flows out through the two outlets provided on the device. Such a design should improve the separating capabilities of the separator markedly. An experimental investigation is underway to evaluate this concept.

Another possible improvement in the oil separation capability of the device can be accomplished by decreasing the static pressure within the separation bubble of the flow. This can be achieved by increasing the centrifugal force on the mixture jet which in turn can be increased by decreasing the radius of the jet center-line. The separation bubble pressure can also be decreased by increasing jet efflux momentum.

#### An Automated Oil Extraction System

It was observed during the feasibility tests that the rate of oil extraction from the oil collecting chambers of the elements affected the quality of oil being extracted appreciably. Too high an extraction rate disturbed the oil-water interface in the collecting chamber and the oil being extracted contained up to 50% water. A low oil extraction rate on the other hand reduced the rate of oil captured by the separation bubble of the flow. This resulted in more oil in the effluents thereby deteriorating the performance of the device. A system to control the oil extraction rate is, therefore, required for proper functioning of the separator. Such a system can be either a proportional or on-off type. Because of the simplicity of their design and their lower costs, systems of the on-off type are considered for this application.

One such system, shown in Figure 15, uses the difference in electrical conductance of water and that of the oil. Practically all oils are electrical insulators. Water (excluding pure water) is capable of conducting electricity. The system of Figure 15 uses this property in sensing the oil-water interface in the collecting chamber by providing two electrodes at different heights in it. For sensing, the electrodes are connected to a 10 volt AC supply through a 1000 ohm resistor. The solenoid valve on the outgoing oil line is operated by the output of the amplifier which receives its input from a rectified voltage signal across the resistor in the sensing circuit. The use of AC supply in the sensing circuit minimizes the electrolysis in the collecting chamber. When the oil-water interface is below the bottom electrode, the resistance in the sensing circuit is very high and practically no current flows through it.

This configuration leads to opening of the solenoid valve provided on the oil outlet line. As the oil is extracted the oil-water interface in the chamber eventually rises above the bottom electrode thereby decreasing the resistance in the sensing circuit. This results in a voltage across the resistor, which when amplified closes the solenoid valve and thus stops the oil extraction. The feasibility of the system will be determined by testing it on the experimental model of the separator.

Alternative means of sensing the oil-water interface may be employed in the foregoing control system. Use of an ultrasonic transducer, although expensive, can sense the oil-water interface precisely. Another means of sensing which can be used is based upon the photo-electric principle. Irrespective of the type of sensing used, the basic design of the control system remains unchanged.

#### COMPARISON WITH THE TYPICAL PARALLEL PLATE SEPARATORS

It was learned from the feasibility tests that a separating device based upon the Coanda-effect principle is capable of gross separation only. Therefore, for an evaluation the separator should be compared with typical, laminar flow parallel plate separators.

Because of its design configuration and the flow velocities through it, the Coanda-effect separator will have a considerably smaller physical size. For instance, a separator to treat 20 gpm of oil-water flow rate can be 1.5 feet long x 1 foot wide x 1.5 feet high; whereas typical parallel plate type separator [1] of the same flow capacity occupies 3 feet--3-1/2 inches x 3 feet--6 inches x 1 foot 7 inches of space. The physical size comparison of the Coanda-effect separators with typical parallel plate type separators for handling 20 and 100 fpm of mixture flow rates is given in Table 2. Because of its smaller size, for a given flow rate, the equipment cost of the Coanda-effect separator will be lower.

Presently, the Coanda-effect separator is in its early stages of development and thus many design modifications are required, therefore, a comparison of its oil separating capabilities with that of the fully developed parallel plate separator is not possible. More work is required before such a comparison can be made. Finally, because of the simplicity of its design, the maintenance of the separator promises to be easier.

Table 2. Physical Size Comparison of the Coanda Effect and Typical Parallel Plate Separators

No.	Maximum Designed Mixture Flow Through the Separator	Coanda-Effect Separator	Parallel Plate Separator
1	20 gpm	1 foot-6 inches long, 1 foot wide, and 1 foot 6 inches high	3 feet-3-1/2 inches long, 3 feet-6 inches wide, and 1 foot-7 in inches high
2	100 gpm	3 feet long, 2 feet wide, and 1 foot-6 inches high	5 feet-9 inches long, 3 feet-6 inches wide, and 3 feet-2 inches high

#### CONCLUSIONS AND RECOMMENDATIONS

1. The investigation conducted to date establishes the feasibility of using the Coanda effect principle in developing an oil-water separator. A separator based upon this concept will be considerably smaller than a laminar-flow separator of comparable capacity.
2. Feasibility tests conducted on an experimental model of the separator, with an oil-water mixture containing 6% oil (mixture flow rate of 1.5 gpm), show that the oil content can be reduced to less than 3%. The extracted oil contained only 5% water. To make the separator practical, staging is necessary.
3. Further, to improve the quality of extracted oil, an automated oil extraction rate controlling system is required. A concept of one such system given should be investigated by testing it on the experimental separator.
4. Improvements in the separating effectiveness of the separator can be accomplished by modifying the velocity distribution of the mixture jet to alter the centrifugal acceleration on it. A conceptual design of such a modification has been formulated.

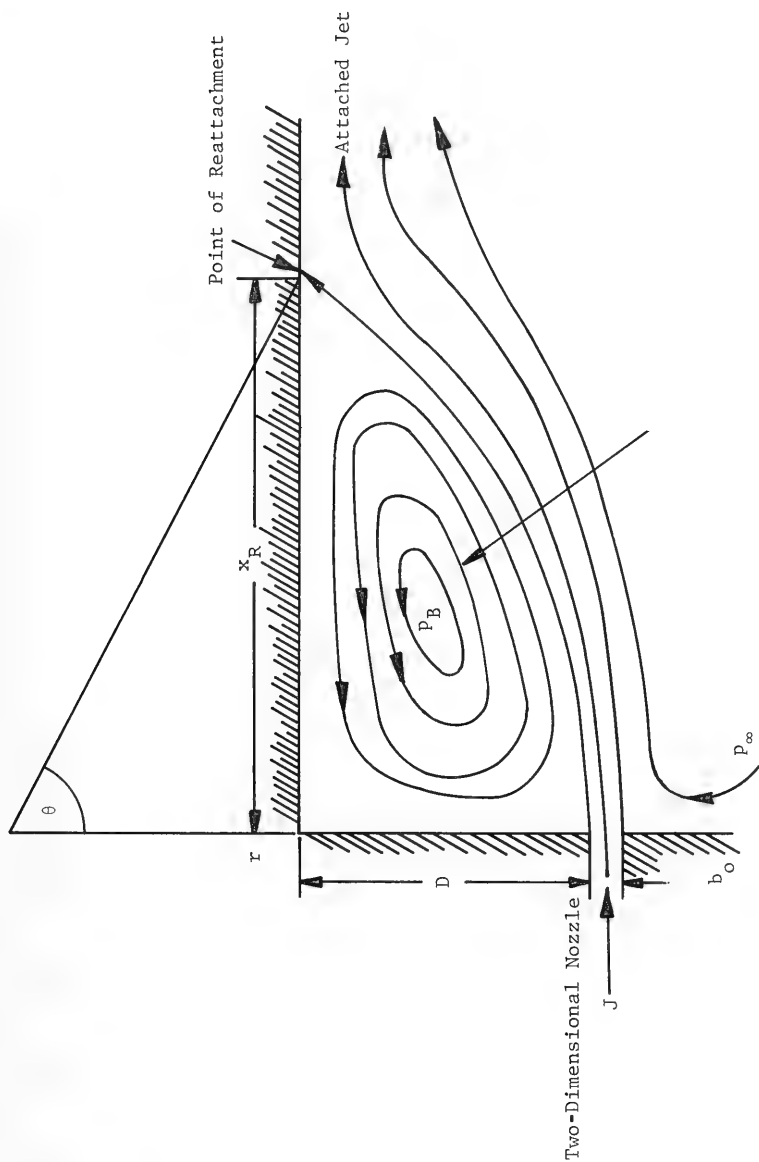


Figure 1. Two-Dimensional Jet Attaching to an Offset Parallel Plate

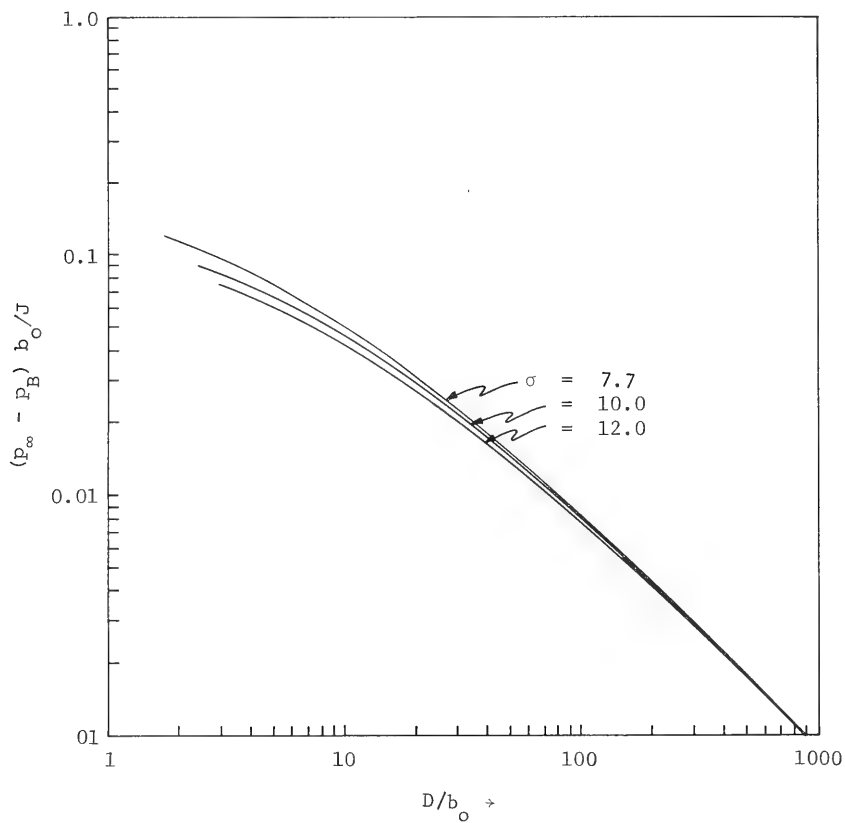
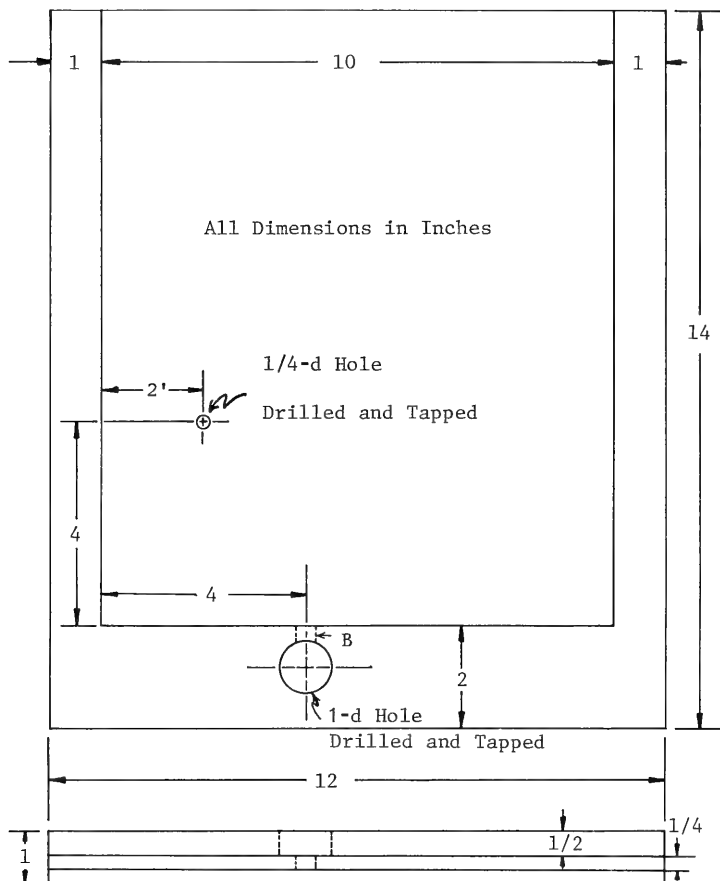


Figure 2. Dimensionless pressure  $(p_\infty - p_B) b_0 / J$  plotted against plate offset parameter  $D/b_0$  for various values of  $\sigma$  of 7.7, 10 and 12.





B is 1/4 inch for Element No. 1  
 B is 3/8 inch for Element No. 2

Figure 3. Sketch of the Test Element.

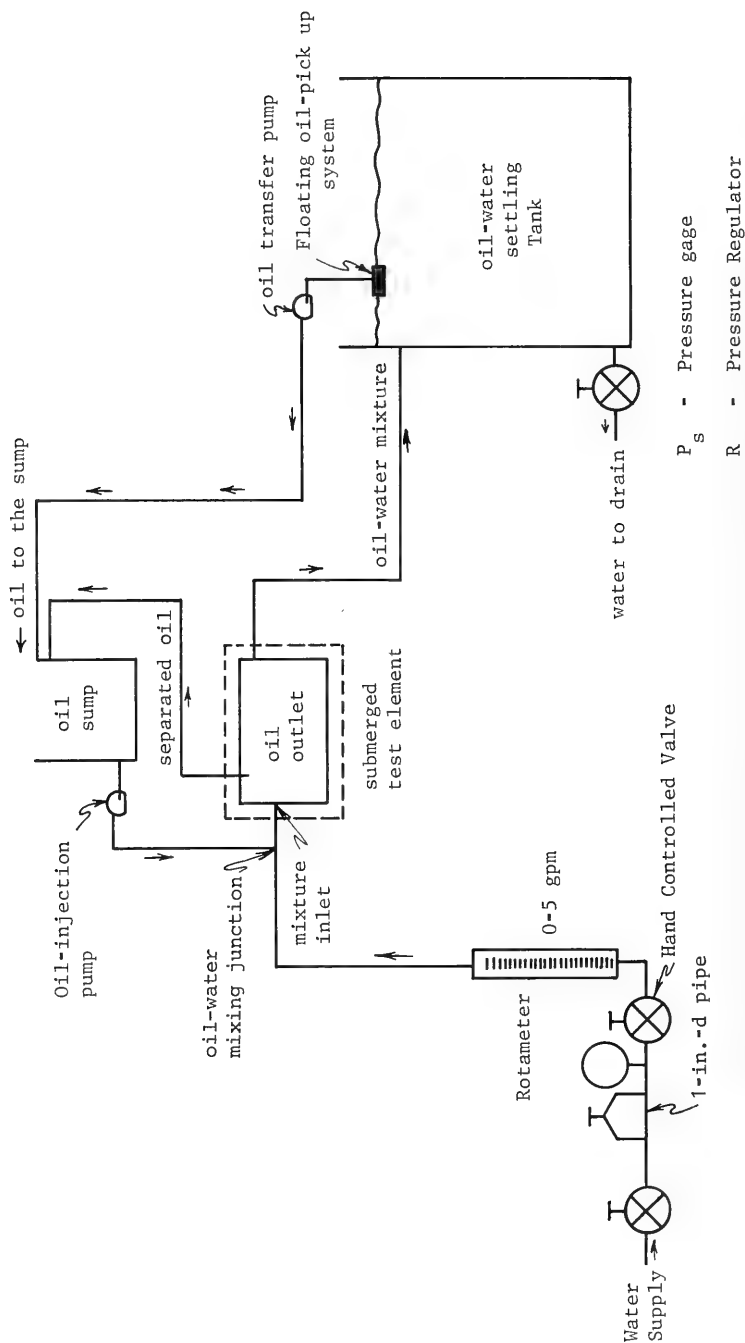


Figure 4. Schematic of the Test Setup.



Figure 5. Flow pattern through Element No. 2 at a mixture flow rate of 1.5 gpm water with 7% oil.

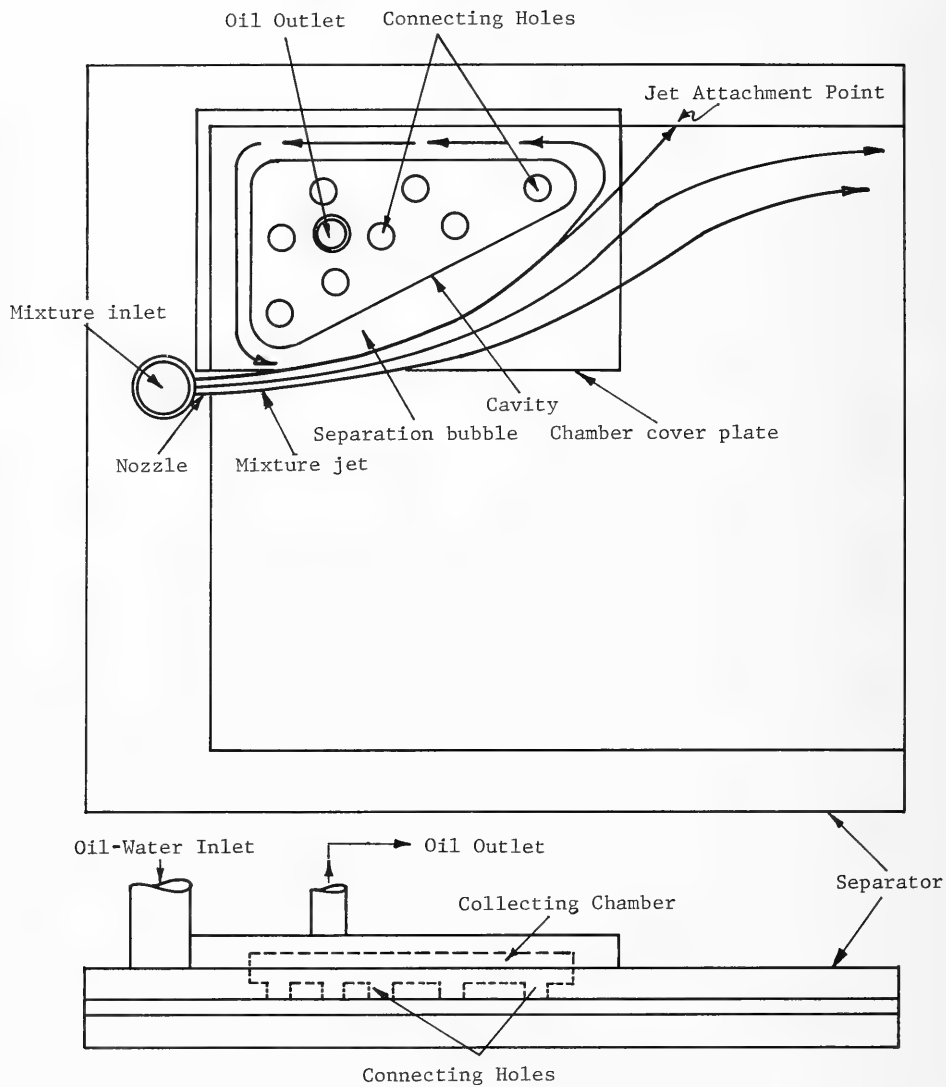


Figure 6. Single Stage Coanda Effect Oil-Water Separator Test Model.

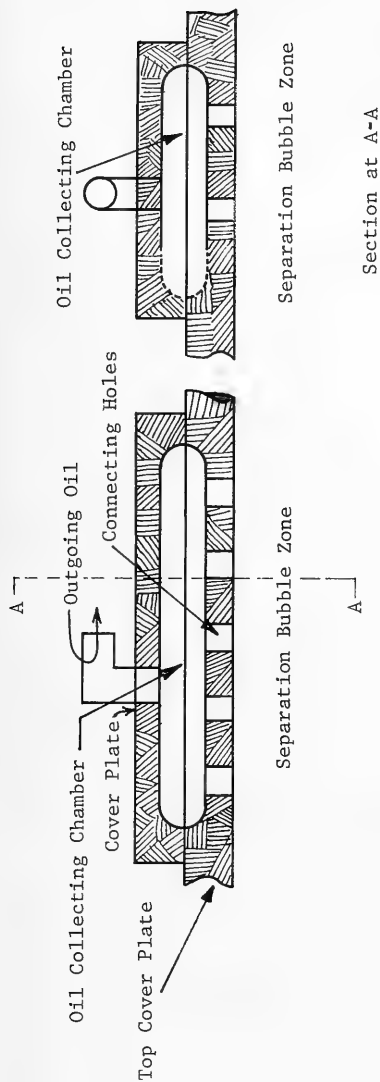


Figure 7. Design features of the oil collecting chamber.

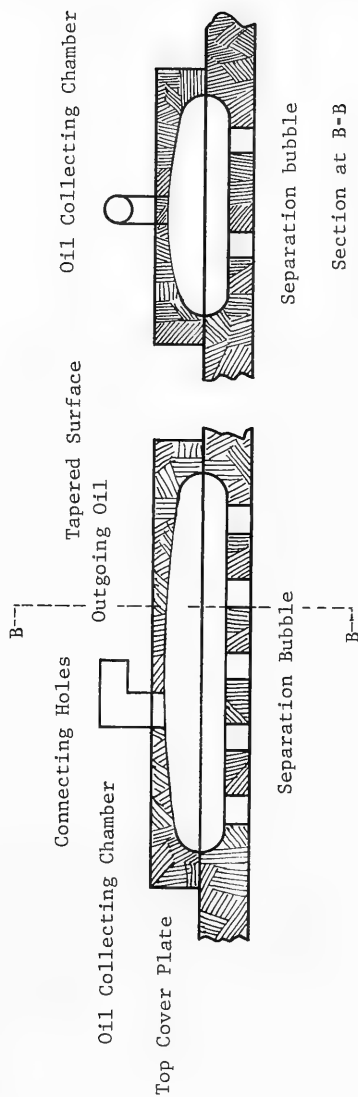
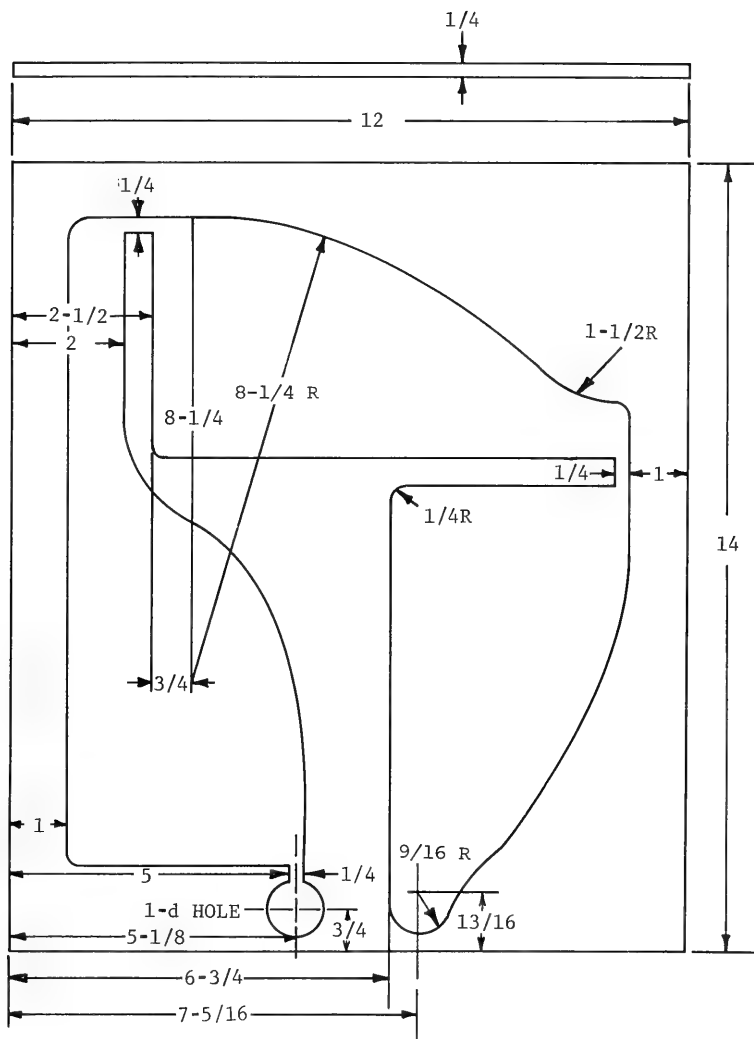


Figure 8. Modified design of the oil collecting chamber.



Figure 9. Flow pattern through the modified element no. 1 at 0.8 gpm water flow rate with 6% oil.



All Dimensions in Inches

Figure 10. The Sketch of Experimental 3-Stage Element

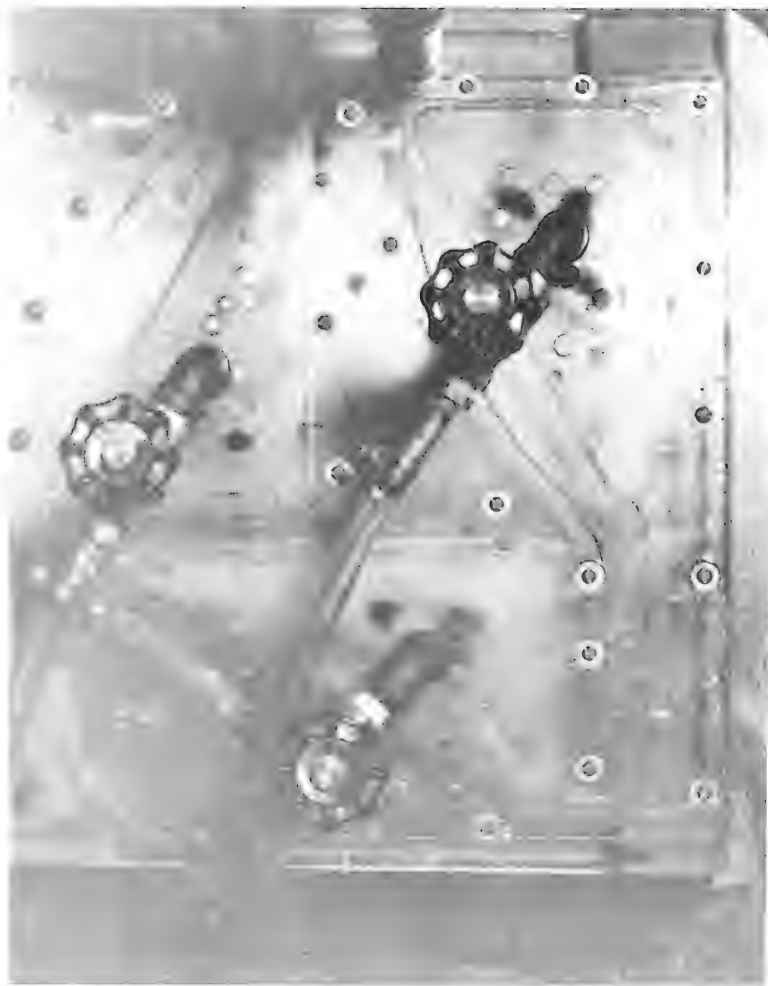


Figure 11. The three-stage test element with water flow only. The flow through device is 0.9 gpm. (The oil droplets in the collecting chambers is the residual oil from the previous tests.)





Figure 12. Flow pattern through the three stage repainting device at 0.9 gpm water flow with 6% oil.

$$u_{\max} = \left[ \frac{3J\sigma}{4\rho(s+s_o)} \right]^{1/2}$$

$$u_{\max} = \frac{3J\sigma}{4\rho(s+s_o)r}$$

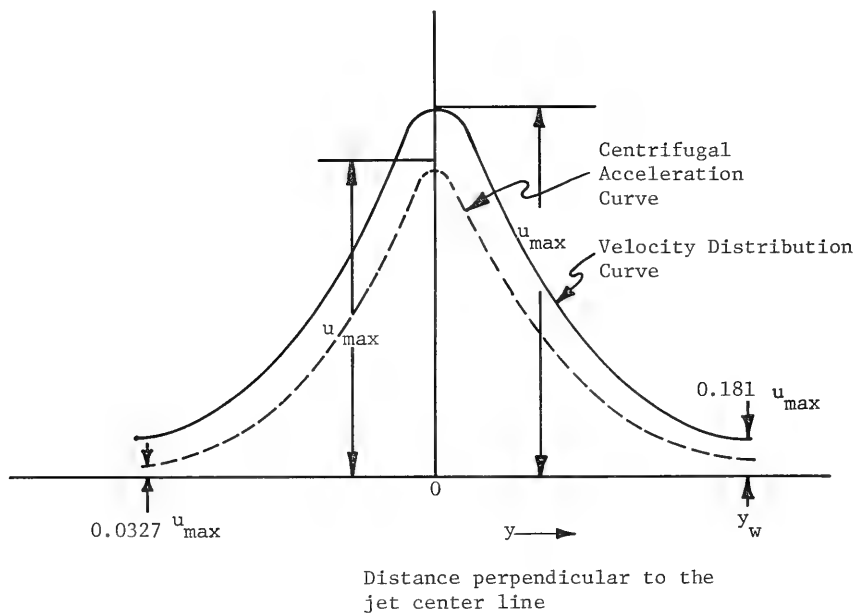


Figure 13. Reattaching Jet Axial Velocity and Centrifugal Acceleration Distributions

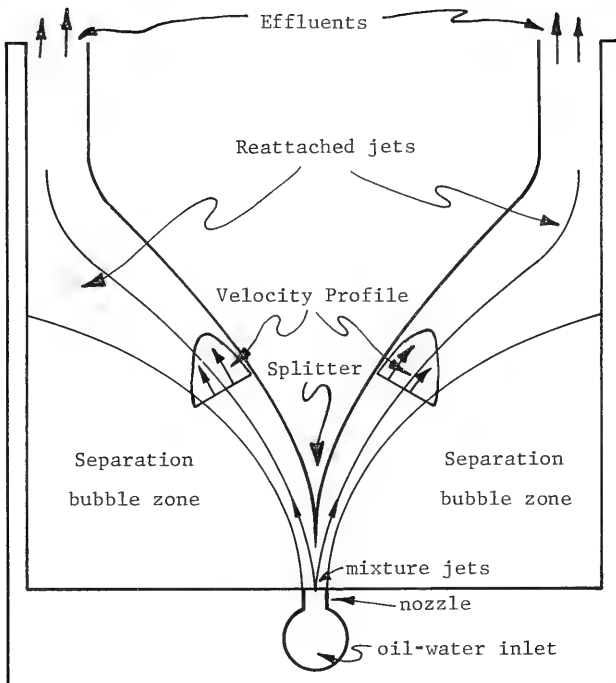


Figure 14. Conceptual Design of a Modified Separator with Improved Jet Velocity Profiles.

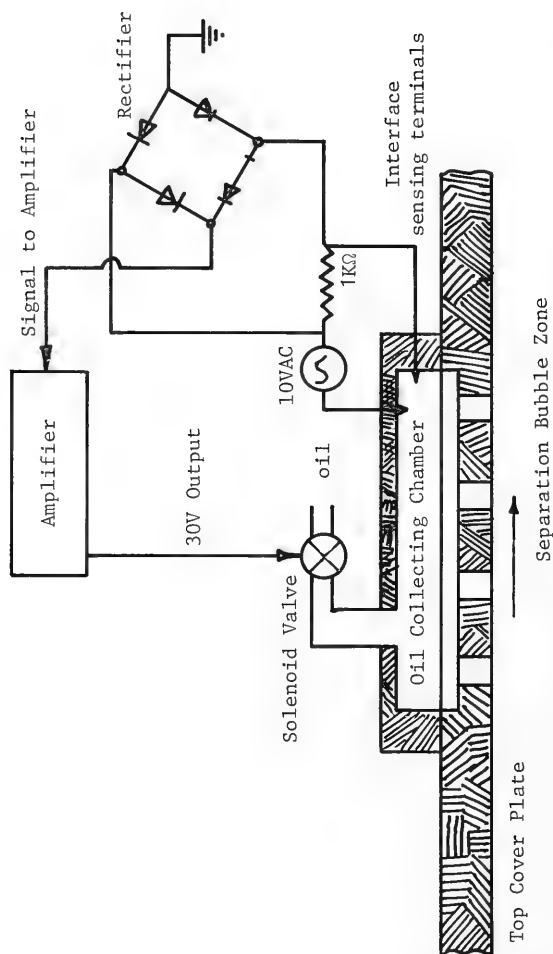


Figure 15. Schematic of an Oil Extraction System

## Appendix A

### EQUATIONS AND DATA DESCRIBING THE FLOW RESULTING FROM A TWO-DIMENSIONAL INCOMPRESSIBLE JET ISSUING PARALLEL TO AN OFFSET FLAT PLATE.

This appendix lists the equations and data describing the flow resulting from a two dimensional incompressible jet issuing parallel to an offset flat plate.

#### Wall Attachment Flow Analysis

This problem has been treated in depth by Bourque and Newman [4], and by Sawyer [5] independently. The analysis conducted by Bourque and Newman is easier to understand and covers a wide range of flow parameters. In this study therefore only the results of Reference 4 were used.

The analysis can be described by considering the flow of a two-dimensional jet issuing from a nozzle in a wall adjacent to a parallel plate with an offset  $D$  as shown in Figure A-1. The jet during its expansion entrains fluid from the surroundings by turbulent action. The entrainment of fluid from the plate side causes a pressure difference across the jet thus curving it toward the plate. If the plate is sufficiently long the jet strikes it and reattaches. The jet divides on striking the plate, sending part of the flow into the separation bubble. The flow equilibrium is reached when the flow entrained by the plate side of the jet is equal to that into the separation bubble from the jet at the point of striking. This is the model used in the analysis of Reference 4. Further, the analysis is based upon the following assumptions:

- (1) The flow is incompressible and two dimensional, i.e., only thin jet sheets are considered.
- (2) The jet efflux velocity is uniform, i.e., the increase in its velocity with the reduced pressure in the separation bubble is neglected. The jet is submerged in a similar fluid and its velocity distribution is that of a free jet.
- (3) The jet entrains the same amount of fluid from each boundary.
- (4) Pressure within the separation bubble is constant and the jet center line is a circular arc up to the point of attachment.
- (5) The force on the plate due to skin friction forces are small and are neglected.

The axial component of jet velocity used is

$$u(s,y) = \left[ \frac{3J\sigma}{4\rho(s+s_0)} \right]^{1/2} \text{Sech}^2 \frac{\sigma y}{s+s_0} \quad (2)$$

where

- $s$  = axial distance from the nozzle,
- $b_0$  = nozzle width,
- $s_0$  = distance of the nozzle from a hypothetical origin of the jet where the flow originates,
- $y$  = co-ordinate normal to the jet center line,
- $\sigma$  = jet spread parameter, to be determined experimentally, it has a value of 7.7 for a turbulent free jet,
- $s_0 = \sigma b_0 / 3$  (see Reference 4).

Before going any further some quantities must be defined as follows:

- $P_\infty$  = free stream pressure
- $p_B$  = Static pressure within the separation bubble
- $r$  = radius of the center line of the reattached jet,
- $\rho$  = density of the fluid,
- $\theta$  = Angular location of the point of reattachment from the nozzle,
- $D$  = distance of the plate from the nozzle axis,
- $x_R$  = distance of the point of attachment from the corner,
- $l$  = length of the plate
- $J$  = jet momentum per unit span of the nozzle.

The equation of the reattaching streamline is given by

$$\frac{3s}{\sigma b_0} = (1/t^2) - 1 \quad (A-1)$$

$$\text{where } t = \tanh \frac{\sigma y}{s + s_0} \quad (A-2)$$

$$\text{if } t = t_1 \quad (A-3)$$

$$\text{where } t_1 = \tanh \frac{\sigma y_1}{s_1 + s_0} \quad (\text{A-4})$$

is the value of  $t$  at the point of reattachment, then the radius of the jet center line is derived from

$$r/b_0 = \frac{\sigma(1/t_1^2 - 1)}{3\theta} \quad (\text{A-5})$$

where  $t_1$  and  $\theta$  are determined from the following equations:

$$D/b_0 = \frac{\sigma(1/t_1^2 - 1)(1 - \cos \theta)}{3\theta} - \frac{1}{2} \quad (\text{A-6})$$

and

$$\cos \theta = 3/2 t_1 - 1/2 t_1^3 \quad (\text{A-7})$$

The half width of the jet at the reattachment point, i.e.,  $y$ , can be easily derived from Equation A-4 and is

$$y_1/b_0 = 1/3 t_1^2 \tanh^{-1} t_1 \quad (\text{A-8})$$

Further, the distance of the reattachment point from the plane of the nozzle is

$$x_R/b_0 = \frac{\sigma(1/t_1^2 - 1) \sin \theta}{3\theta} - \frac{\tanh^{-1} t_1}{3t_1^2 \sin \theta} \quad (\text{A-9})$$

Finally, the mean pressure within the separation bubble is computed by

$$p_\infty - p_B = J/b_0 \left[ \frac{3\theta}{\sigma(1/t_1^2 - 1)} \right] \quad (\text{A-10})$$

A wall attachment element can be designed using Equations (A-1) through (A-9).

However, to use these equations conveniently, it is required that the flow parameters  $x_R/b_0$ ,  $r/b_0$ ,  $y_1/b_0$  and  $\theta$  be known as functions of the pre-determined parameter  $D/b_0$ . These equations are complex and can not be expressed explicitly in terms of  $D/b_0$  alone.

A numerical scheme was devised to compute  $x_R/b_0$ ,  $r/b_0$ ,  $y_1/b_0$  for known values of  $D/b_0$ . The numerical method runs as follows. By inspection of Equation A-7, maximum and minimum values of  $t_1$  which render  $\theta$  between 90 degrees and 30 degrees were determined. Since  $y_1$  is positive, only positive values of  $r_1$  must be considered. Further, it was determined from Equation A-7 that for  $\theta$  to lie between 90 degrees and 30 degrees,  $t_1$  must range between 0 and 0.50. A known value of  $t_1$  yields  $\theta$  from Equation A-7. For a selected value of  $\sigma$  with known  $t_1$  and  $\theta$ , parameters  $D/b_0$ ,  $r/b_0$ ,  $y_1/b_0$  and  $x_R/b_0$  can be determined from Equations A-6, A-5, A-8 and A-10 respectively. Thus computing a set of values for  $x_R/b_0$ ,  $r/b_0$  and  $y_1/b_0$  for a known  $D/b_0$ . A series of similar sets were computed by increasing  $t_1$  by 0.05 each time up to a final value of 0.50. A total of three series of sets were computed for different  $\theta$  of 12, 10 and 7.7 respectively.

For easy usage the parameters  $\theta$ ,  $y_1/b_0$ ,  $r/b_0$  and  $x_R/b_0$  were plotted against  $D/b_0$  for values of  $D/b_0$  ranging from 1 to 1000. These plots are shown in Figures A-2 through A-5. It should be added here that flow parameters become independent of the parameter  $D/b_0$  for  $D/b_0$  greater than 35. Also the analysis becomes inaccurate for  $D/b_0$  less than 3. Further, the value of  $\sigma$ , the spread parameter chosen can affect the flow parameters appreciably.

One last remark of interest is regarding the value of  $\sigma$ , the spread parameter to be used while using these curves. Because of the curvature effect a  $\sigma$  of 7.7 does not apply. It is reported in Reference 1 that a value of 12 for  $\sigma$  gives flow parameters values that are in fair agreement with the experimental data.



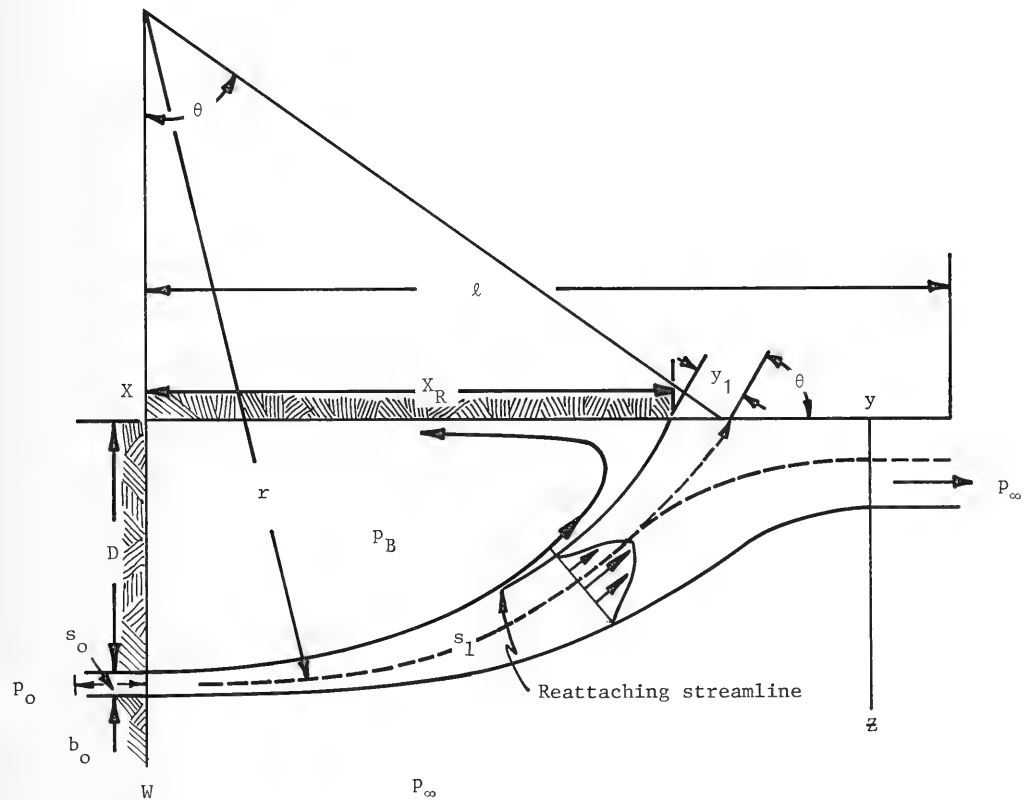


Figure A-1. A two-dimensional jet reattached to an offset parallel plate.

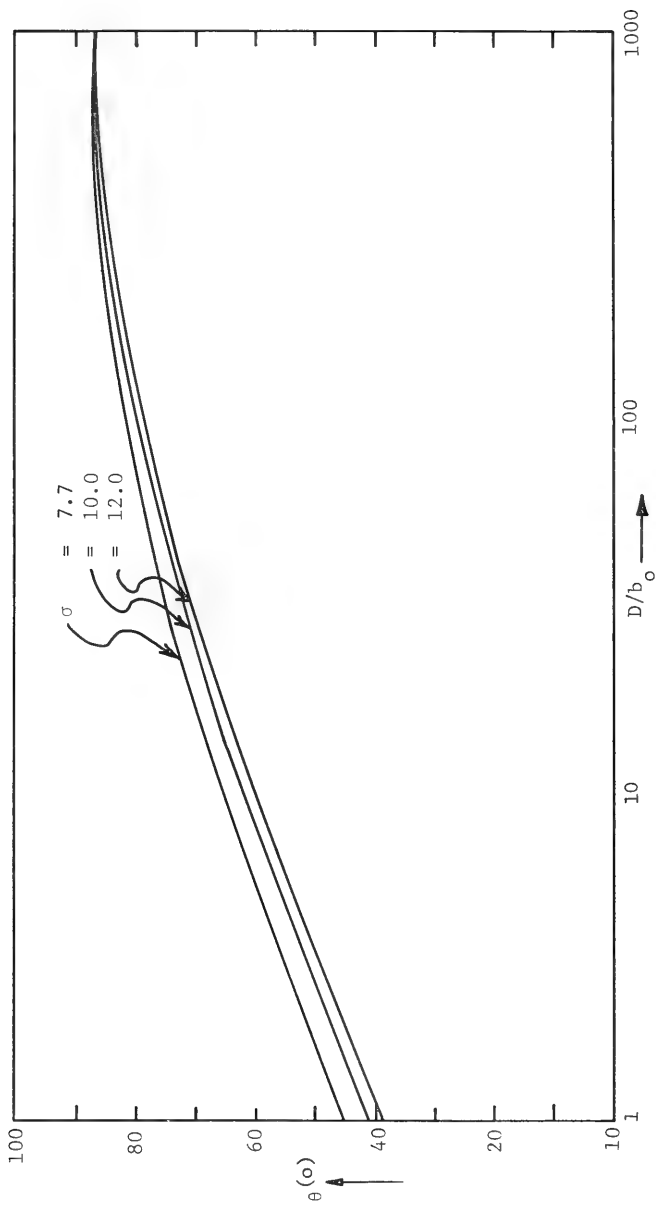


Figure A-2. Angular location ( $\theta$ ) of the jet reattachment point plotted against plate offset parameter  $D/b_0$  for various values of  $\sigma$  of 7.7, 10 and 12.

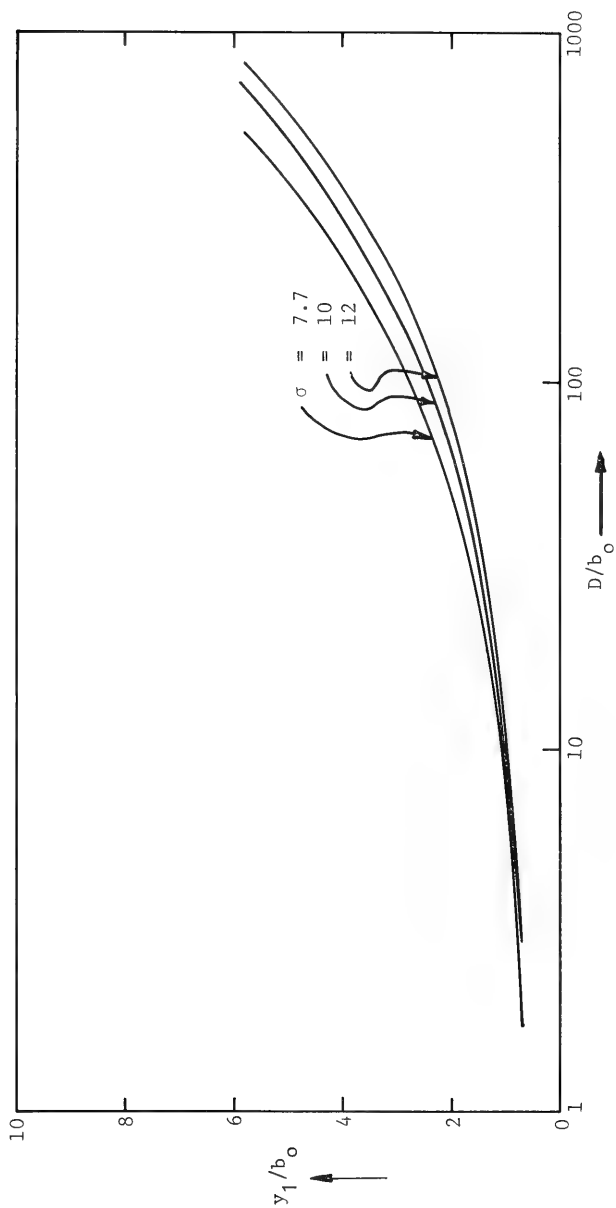


Figure A-3. Half-width ( $y_1/b_0$ ) of the jet at the reattachment point plotted against plate offset parameter  $D/b_0$  for various values of  $\sigma$  of 7.7, 10 and 12.

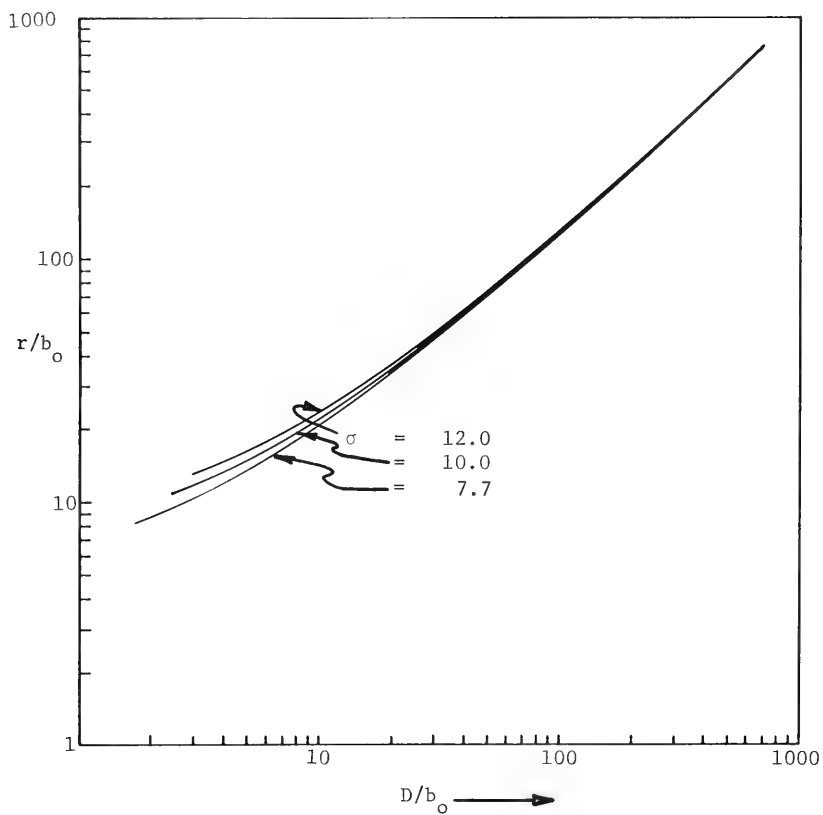


Figure A-4. Jet center line radius  $r/b_0$  plotted against plate offset  $D/b_0$  for various values of  $\sigma$  of 7.7, 10 and 12.

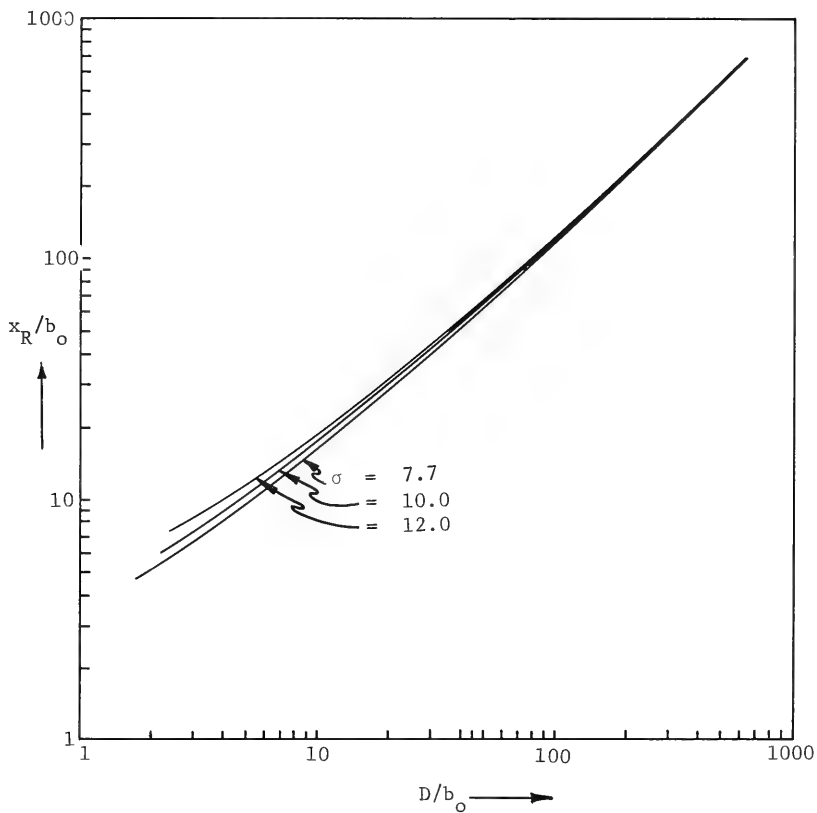


Figure A-5. Reattachment distance  $x_R/b_o$  plotted against plate offset for various values of  $\sigma$  of 7.7, 10 and 12.

## Appendix B

### SPECIFICATIONS OF OIL USED IN THE TEST MIXTURE AND THE OIL INSPECTION PUMP

This appendix lists the specification of

- (a) the oil used in the test mixture
- (b) the oil inspection pump

Hydraulic Fluid - Petroleum Base

Mil. spec.: MIL-H-5606C

Fed. Stock No.: FSN 9150-223-4134

Specific gravity: 0.88 to 0.90

Color: red

Kinematic viscosity: 8.0 stokes at 40 degrees F  
to 0.10 stokes at 130 degrees F

Oil Injection Pump

Fluid Metering Corp

FMI Model RRP-F

with 3/8-inch piston, 0-100 cc/min at 50 psi. Variable flow  
with micrometer flow adjustment head. Electric motor drive.  
115V, 4.5A at 60 cycles, 1725 rpm.

### ACKNOWLEDGMENTS

John B. Curry assisted in the laboratory tests of the  
experimental elements

### REFERENCES

1. Naval Civil Engineering Laboratory. Mechanical and electrical  
engineering department, letter report, YF38.554.001.01.001:  
Program plan for oily waste handling at navy shore establishment,  
by E.L. Ghormley, Ph.D., Port Hueneme, California, June 1972.
2. S.M. Finger and R.B. Tabakin, Development of shipboard  
oil/water separation systems, ASME paper 73-ENAS-38, presented  
at the intersociety conference on Environmental Systems, San  
Diego, California, July 16-19, 1973.
3. U.S. Navy Case 56,734: Patent application on coanda effect  
oil-water separator, by A.J. Paszyc, Ph.D., D. Pal and J.B. Curry,  
15 June 1973.

4. C. Bourque and B.G. Newman, Reattachment of a two-dimensional incompressible jet to an adjacent flat plate, the Aeronautical Quarterly, Vol XI, Aug, 1960, pp. 201-232.
5. R.A. Sawyer, The flow due to a two dimensional jet issuing parallel to a flat plate, J. Fluid Mech. Vol 9, 1960, pp. 543-60.
6. Naval Civil Engineering Laboratory. Contract Report CR 73.015: Test and evaluation of oil-water separation systems by the Ben Holt Co., Pasadena, California, Port Hueneme, California, 8 Nov. 1972.

# DISTRIBUTION LIST

SNDL Code	No. of Activities	Total Copies	
--	1	12	Defense Documentation Center
--	1	1	Director of Navy Laboratories
FKAIC	1	3	Naval Facilities Engineering Command
FKN1	6	6	NAVFAC Engineering Field Divisions
FKN5	9	9	Public Works Centers
FA25	1	1	Public Works Center
--	9	9	RDT&E Liaison Officers at NAVFAC Engineering Field Divisions and Construction Battalion Centers
--	298	298	CEL Special Distribution List No. 8 for persons and activities interested in reports on Mechanical Systems

Natick Labs \*  
Kansas St.  
Natick, MA 01761

Commanding Officer (Code 200)  
Navy Public Works Center  
Naval Base  
Newport, RI 02840

Public Works Officer  
Portsmouth Naval Shipyard  
Portsmouth, NH 03801

Public Works Officer  
Boston Naval Shipyard  
Boston, MA 02129

Commanding Officer  
Naval Supply Depot  
Newport, RI 02840

Public Works Officer  
U.S. Naval Disciplinary Command  
Portsmouth, NH 03801

Public Works Officer  
Naval Hospital, Boston  
Chelsea, MA 02150

President  
Naval War College  
Code 22  
Newport, RI 02840

Public Works Officer  
Naval Air Station  
Brunswick, ME 04011

Dr. E. M. Lenoe  
Army Materials & Mechanics Research Center  
Bldg 39, Room 412  
Arsenal Street  
Watertown, MA 02172

Commanding Officer  
U.S. Naval Station  
Naval Base  
Newport, RI 02840

Public Works Officer  
Naval Radio Station (T), Cutler  
East Machias, ME 04630

Public Works Officer  
Naval Air Station  
South Weymouth, MA 02190

Staff Civil Engineer  
Naval Supply Center  
Newport, RI 02840

Facilities Officer  
Code NA 2  
New London Laboratory  
Naval Underwater Systems Center  
New London, CT 06320

LCDR David A. Cacchione, USN  
Office of Naval Research, Broff  
495 Summer Street  
Boston, MA 02210

Mr. S. Milligan  
SB 322  
Naval Underwater Systems Center  
Newport, RI 02844

Public Works Department  
Box 400  
Naval Submarine Base, New London  
Groton, CT 06340

Public Works Officer  
Naval Facility  
Nantucket, MA 02554

Public Works Officer  
Naval Underwater Systems Center  
Newport, RI 02844

Commanding General  
U. S. Army Electronics Command  
Attn: AMSEL-GG-TD  
Fort Monmouth, NJ 07703

Public Works Officer  
Naval Air Station  
Quonset Point, RI 02819

Commanding Officer  
CBC Technical Library  
Naval Construction Battalion Center  
Davisville, RI 02854 (2 copies)

Public Works Officer  
Naval Air Propulsion Test Center  
Trenton, NJ 08628

\* All addressees receive one copy unless otherwise indicated.



Public Works Officer  
Naval Air Station  
Lakehurst, NJ 08733

Commanding Officer  
Mobile Construction Battalion 74  
FPO New York 09501

Public Works Officer  
U. S. Naval Support Force Antarctica  
FPO New York 09501

Commanding Officer  
Amphibious Construction Battalion TWO  
FPO New York 09501

Public Works Officer  
U.S. Naval Activities, United Kingdom  
FPO New York 09510

Public Works Officer  
U.S. Naval Activities, United Kingdom Det.  
FPO New York 09510

Public Works Officer  
U. S. Naval Communication Station  
FPO New York 09512

Public Works Officer  
U. S. Naval Security Group Activity  
FPO New York 09518

Public Works Officer  
U. S. Naval Air Facility  
FPO New York 09520

Public Works Officer  
U.S. Naval Support Activity  
FPO New York 09521

Director  
European Branch-Atlantic Division  
Naval Facilities Engineering Command  
Naval Support Activity-Box 51  
FPO New York 09521

Public Works Officer  
U. S. Naval Air Facility  
FPO New York 09523

Public Works Officer  
U. S. Naval Communication Station  
FPO New York 09525

Public Works Officer  
U.S. Naval Control of Shipping Office  
FPO New York 09526

Public Works Officer  
U. S. Naval Medical Research Unit No. 3  
FPO New York 09527

Public Works Officer  
U.S. Navy Fleet Support Office  
FPO New York 09532

LT Ronald A. Milner, CEC, USN  
U. S. Naval Station  
Box 9  
FPO New York 09540

Public Works Officer  
Morocco-U. S. Naval Training Command  
Box 19  
FPO New York 09544

Public Works Officer  
U. S. Naval Communication Station  
Box 41  
FPO New York 09544

Public Works Officer  
U.S. Navy Support Activity  
FPO New York 09550

Public Works Officer  
U.S. Naval Station  
FPO New York 09551

Commanding Officer  
U.S. Naval Hospital  
FPO New York 09551

Public Works Officer  
U. S. Naval Facility  
FPO New York 09552

Public Works Officer  
U. S. Naval Facility  
FPO New York 09553

Public Works Officer  
U.S. Naval Communication Station  
FPO New York 09554

Public Works Officer  
U.S. Naval Security Group Activity  
FPO New York 09555

Public Works Officer  
U. S. Naval Facility  
FPO New York 09558

Public Works Officer  
U. S. Naval Air Station  
FPO New York 09560

Public Works Officer  
U. S. Naval Station  
FPO New York 09571

Public Works Officer  
U. S. Naval Communication Station  
FPO New York 09580

Public Works Officer  
U. S. Naval Support Activity  
FPO New York 09585

Public Works Officer  
U. S. Naval Station  
Box 25  
FPO New York 09593

Public Works Officer  
U. S. Naval Station  
Box 6  
FPO New York 09597

Public Works Officer  
U. S. Naval Communication Station  
APO New York 09843

Public Works Officer, Naval Station  
136 Flushing Avenue  
Brooklyn, NY 11251

Public Works Officer  
Naval Strategic Systems Navigation Facility  
Flushing & Washington Avenue  
Brooklyn, NY 11251

Public Works Officer  
U. S. Naval Hospital  
St. Albans, LI, NY 11425

Public Works Officer  
Naval Ships Parts Control Center  
Mechanicsburg, PA 17055

Public Works Officer  
Naval Air Development Center  
Warminster, PA 18974

Public Works Officer  
Naval Air Station  
Willow Grove, PA 13090

Commanding Officer  
Code 016A  
Northern Division  
Naval Facilities Engineering Command  
Philadelphia, PA 19112

RDT&E Liaison Officer  
Code 102 Northern Division  
Naval Facilities Engineering Command  
Philadelphia, PA 19112

Public Works Officer  
Philadelphia Naval Shipyard  
Philadelphia, PA 19112

Commanding Officer  
Naval Station  
Philadelphia, PA 19112

Public Works Officer  
Naval Air Engineering Center  
Philadelphia, PA 19112

Public Works Officer  
Naval Hospital  
17th Street & Pattison Avenue  
Philadelphia, PA 19145

Public Works Officer  
National Naval Medical Center  
Bethesda, MD 20014

Mr. R. B. Allnutt  
Code 1706  
Naval Ship Research & Development Center  
Bethesda, MD 20034

Head Facilities & Industrial Department  
Code 54  
Carderock Laboratory  
Naval Ship Research & Development Center  
Bethesda, MD 20034

William F. Gerhold  
National Bureau of Standards  
Corrosion Section  
Washington, DC 20234

Chief of Engineers  
U. S. Army  
DAEN-MCE-D  
Washington, DC 20314

Commander  
Naval Ship Systems Command  
Code OOC  
Washington, DC 20362

Mr. David L. Southey  
Code 41A  
Bureau of Medicine and Surgery  
Navy Department  
Washington, DC 20372

U.S. Naval Oceanographic Office  
Library - Code 3600  
Washington, DC 20373

Director  
Naval Research Laboratory  
Code 2627  
Washington, DC 20375

Public Works Officer  
Naval Research Laboratory  
455 Overlook Ave., SW  
Washington, DC 20375

Director of Navy Laboratories  
Room 300, Crystal Plaza Bldg 5  
Department of the Navy  
Washington, DC 20376

Commanding Officer  
Chesapeake Division - Code 03  
Naval Facilities Engineering Command  
Washington Navy Yard  
Washington, DC 20390

Director, Design Division - 04  
Chesapeake Division  
Naval Facilities Engineering Command  
Washington Navy Yard  
Washington, DC 20390

Public Works Officer  
Naval Air Facility  
Washington, DC 20390

Commandant  
Naval District Washington  
Public Works Department - Code 412  
Washington, DC 20390

Public Works Officer  
Naval Security Station  
3801 Nebraska Avenue, NW  
Washington, DC 20390

Public Works Officer  
Naval Communication Station  
Washington, DC 20390

Mr. M. R. Whitley  
Criteria & Research Branch  
Office of Construction Management  
General Services Administration  
Washington, DC 20405

Commanding Officer  
Naval Explosive Ordnance  
Disposal Facility - Code TI 1  
Indian Head, MD 20640

Public Works Officer  
Naval Ordnance Station  
Indian Head, MD 20640

Public Works Officer  
Naval Air Station  
Patuxent River, MD 20670

Commander  
Naval Ship Engineering Center  
Code 6136  
Prince Georges Center  
Hyattsville, MD 20782

Commander  
Naval Ship Engineering Center  
Code 6162  
Prince Georges Center  
Hyattsville, MD 20782

Technical Library  
Naval Ship Engineering Center  
622 Center Bldg  
Prince Georges Center  
Hyattsville, MD 20782

Chief  
Marine & Earth Sciences Library  
National Oceanic & Atmospheric Admin.  
Dept of Commerce  
Rockville, MD 20852

M. E. Ringenbach  
Engineering Development Lab (C61)  
National Oceanic & Atmospheric Admin.  
National Ocean Survey  
Rockville, MD 20852

Public Works Officer  
Naval Ordnance Laboratory, White Oak  
Code 942  
Silver Spring, MD 20910

Commanding Officer  
ATTN: STEAP-TL  
Bldg 305  
Aberdeen Proving Ground, MD 21005

Director  
Division of Engineering & Weapons  
U. S. Naval Academy  
Annapolis, MD 21402

Dr. Neil T. Monney  
Naval Systems Engineering Dept  
U. S. Naval Academy  
Annapolis, MD 21402

Public Works Department  
U. S. Naval Academy  
Annapolis, MD 21402

Library, Code 5642  
Annapolis Laboratory  
Naval Ship Research & Dev. Center  
Annapolis, MD 21402

Public Works Officer  
Naval Support Facility  
Box 277  
Thurmont, MD 21788

U.S. Army Coastal Eng. Research Center  
Kingman Building  
Fort Belvoir, VA 22060

Public Works Officer  
Marine Corps Dev. Education Command  
Quantico, VA 22134

Facilities Officer  
Office of Naval Research  
Code 108  
800 North Quincy Street  
Arlington, VA 22217

Dr Nicholas Perrone  
Code 439  
Office of Naval Research  
800 North Quincy Street  
Arlington, VA 22217

Oceanographer of the Navy  
ATTN: Code N712  
200 Stovall Street  
Alexandria, VA 22332

CAPT Pharo A. Phelps, CEC, USN  
Naval Facilities Engineering Command  
200 Stovall Street  
Alexandria, VA 22332

Commander  
Code 0436B  
Naval Facilities Engineering Command  
200 Stovall Street  
Alexandria, VA 22332

Public Works Officer  
Naval Weapons Laboratory  
Dahlgren, VA 22448

Public Works Officer  
Fleet Combat Direction Systems  
Training Center, Atlantic  
Dam Neck  
Virginia Beach, VA 23461

Public Works Officer  
Naval Weapons Station  
Yorktown, VA 23491

Commanding Officer  
Navy Public Works Center  
Norfolk, VA 23511

Staff Civil Engineer  
Naval Air Station  
Norfolk, VA 23511

RDT&E Liaison Officer  
Code 09P2  
Atlantic Division  
Naval Facilities Engineering Command  
Norfolk, VA 23511 (2 copies)

Director  
Amphibious Warfare Board  
Naval Amphibious Base, Little Creek  
Norfolk, VA 23521

Public Works Officer  
Naval Amphibious Base, Little Creek  
Norfolk, VA 23521

General Engineer  
Naval Hospital  
Portsmouth, VA 23708

Director  
Engineering Division - Code 440  
Public Works Department  
Norfolk Naval Shipyard  
Portsmouth, VA 23709

Public Works Officer  
Naval Facility, Cape Hatteras  
Buxton, NC 27920

Public Works Officer  
Marine Corps Air Station  
Cherry Point, NC 28533

Public Works Officer  
Marine Corps Air Station, New River  
Jacksonville, NC 28540

Public Works Officer  
Marine Corps Base  
Camp Lejeune, NC 28542

Public Works Officer  
Charleston Naval Shipyard  
Naval Base  
Charleston, SC 29408

Staff Civil Engineer  
Naval Hospital  
Charleston, SC 29408

Public Works Officer  
Naval Station  
Naval Base  
Charleston, SC 29408

RDT&E Liaison Officer  
Southern Division - Code 90  
Naval Facilities Engineering Command  
P. O. Box 10068  
Charleston, SC 29411

Staff Civil Engineer  
Naval Supply Center  
Charleston, SC 29411

Public Works Officer  
Naval Hospital  
Beaufort, SC 29902

Public Works Officer  
Marine Corps Air Station  
Beaufort, SC 29902

Public Works Officer  
P. O. Box 35  
Marine Corps Recruit Depot  
Parris Island, SC 29905

Public Works Officer  
Naval Air Station, Atlanta  
Marietta, GA 30063

Public Works Officer  
Navy Supply Corps School  
Athens, GA 30601

Public Works Department  
Naval Air Station  
Glynco, GA 31520

Public Works Officer  
Naval Air Station  
Albany, GA 31703

Public Works Officer  
Marine Corps Supply Center  
Albany, GA 31704

Director of Engineering  
Naval Air Station  
Jacksonville, FL 32212

Public Works Officer  
Naval Air Station  
Cecil Field, FL 32215

AFCEC/DE  
Tyndall Air Force Base, FL 32401

R. E. Elliott  
Code 710  
Naval Coastal Systems Laboratory  
Panama City, FL 32401

Public Works Officer  
Naval Coastal Systems Laboratory  
Panama City, FL 32401

Staff Civil Engineer  
Naval Air Station  
Pensacola, FL 32508

Commanding Officer (Code 200)  
Navy Public Works Center, Bldg 1  
Naval Air Station  
Pensacola, FL 32508

Public Works Officer  
Naval Air Station, Whiting Field  
Milton, FL 32570

Public Works Officer  
Naval Training Center  
Orlando, FL 32813

Staff Civil Engineer  
Naval Training Equipment Center  
Orlando, FL 32813

Public Works Officer  
Naval Security Group Activity  
Homestead, FL 33030

Public Works Officer  
Naval Station  
Key West, FL 33040

Staff Civil Engineer  
Naval Air Station  
Key West, FL 33040

Public Works Officer  
Naval Air Station, Memphis (84)  
Millington, TN 38054

Staff Civil Engineer  
Naval Hospital Memphis  
Millington, TN 38054

Public Works Officer  
Naval Air Station  
Meridian, MS 39301

Public Works Officer  
Naval Ordnance Station  
Louisville, KY 40214

AFIT  
Civil Engineering School  
Wright-Patterson AFB, OH 45433

Public Works Officer  
Naval Avionics Facility  
Indianapolis, IN 46218

Public Works Officer  
Naval Ammunition Depot  
Crane, IN 47522

Public Works Officer  
Naval Air Facility, Detroit  
Mount Clements, MI 48043

Public Works Officer  
Naval Air Station  
Glenview, IL 60026

Army Construction Eng. Research Lab.  
ATTN: Library  
P. O. Box 4005  
Champaign, IL 61820

Commanding Officer - Engineering Div.  
MRD-Corps of Engineers  
Department of the Army  
P. O. Box 103, Downtown Station  
Omaha, NE 68101

Public Works Department  
Maintenance Division  
Naval Air Station, New Orleans  
Belle Chasse, LA 70037

Public Works Officer  
Naval Air Station, New Orleans  
Belle Chasse, LA 70037

Public Works Officer  
Naval Ammunition Depot  
McAlester, OK 74501

Public Works Officer  
Naval Air Station  
Dallas, TX 75211

Public Works Officer  
Naval Air Station  
Chase Field  
Beeville, TX 78102

Public Works Officer  
Naval Air Station  
Corpus Christi, TX 78419

Public Works Department  
Marine Corps Air Station  
Yuma, AZ 85364

Technical Reference Division  
Headquarters, Fort Huachuca  
Fort Huachuca, AZ 85613

AFWL  
CE Division  
Kirtland AFB, NM 87117

Public Works Officer  
Naval Ordnance Missile Test Facility  
White Sands Missile Range, NM 88002

Public Works Officer  
Naval Air Station  
Fallon, NV 89406

Public Works Officer  
Naval Ammunition Depot  
Hawthorne, NV 89415

Public Works Officer  
Naval Air Station  
Los Alamitos, CA 90720

Public Works Officer  
Naval Weapons Station  
Seal Beach, CA 90740

Public Works Officer  
Naval Station  
Long Beach, CA 90801

Dr Arthur R. Laufer  
Office of Naval Research, BROFF  
1030 East Green Street  
Pasadena, CA 91106

Officer in Charge  
Pasadena Laboratory - Naval Undersea Center  
ATTN: Technical Library  
3202 E. Foothill Blvd  
Pasadena, CA 91107

Asst. Public Works Officer  
Naval Weapons Station  
Fallbrook Annex  
Fallbrook, CA 92028

Staff Civil Engineer  
Naval Air Station  
Imperial Beach, CA 92032

Public Works Officer  
Marine Corps Base  
Camp Pendleton, CA 92055

Dr J. D. Stachiw  
Code 6505  
Naval Undersea Center  
San Diego, CA 92132

Mr. R. E. Jones  
Code 65402  
Naval Undersea Center  
San Diego, CA 92132

Technical Library  
Code 1311  
Naval Undersea Center  
San Diego, CA 92132

Public Works Officer  
Code 75  
Naval Undersea Center  
San Diego, CA 92132

Staff Civil Engineer  
Naval Training Center  
San Diego, CA 92133

Public Works Officer  
Naval Administrative Command  
Naval Training Center  
San Diego, CA 92133

Civil Staff Engineer  
Naval Hospital  
San Diego, CA 92134

Public Works Officer  
Naval Air Station  
North Island  
San Diego, CA 92135

Staff Civil Engineer  
Naval Station  
San Diego, CA 92136

Commanding Officer  
Navy Public Works Center  
Naval Base  
San Diego, CA 92136

Public Works Officer  
Naval Air Station  
Miramar  
San Diego, CA 92145

Public Works Officer  
Naval Amphibious Base  
Coronado  
San Diego, CA 92155

Public Works Officer  
Naval Air Facility  
El Centro, CA 92243

Public Works Officer  
Marine Corps Base  
Bldg 1130  
Twentynine Palms, CA 92278

Public Works Officer  
Marine Corps Supply Center  
Barstow, CA 92311

Public Works Department (151)  
Marine Corps Air Station  
El Toro  
Santa Ana, CA 92709

Commanding Officer  
Naval Missile Center  
Code 5632.2, Technical Library  
Point Mugu, CA 93042

Office of Patent Counsel  
Code PC (Box 40)  
Naval Missile Center  
Point Mugu, CA 93042

Public Works Officer  
Naval Air Station  
Point Mugu, CA 93042

Public Works Officer  
Code 82  
Naval Construction Battalion Center  
Port Hueneme, CA 93043

Librarian, Code 9215  
Construction Equipment Department  
Naval Construction Battalion Center  
Port Hueneme, CA 93043

Commander  
31st Naval Construction Regiment  
Naval Construction Battalion Center  
Port Hueneme, CA 93043

Commanding Officer  
Code 155  
Naval Construction Battalion Center  
Port Hueneme, CA 93043

Commanding Officer  
Naval Schools of Construction  
Port Hueneme, CA 93043

Public Works Officer (70)  
Naval Weapons Center  
China Lake, CA 93555

Public Works Officer  
Naval Facility, Big Sur  
Big Sur, CA 93920

Superintendent  
Attn: Library (Code 2124)  
Naval Postgraduate School  
Monterey, CA 93940

Public Works Officer  
Public Works Dept  
Naval Postgraduate School  
Monterey, CA 93940

Dr. Edward B. Thornton  
Department of Oceanography  
Naval Postgraduate School  
Monterey, CA 93940

Public Works Officer  
Naval Air Station  
Moffett Field, CA 94035

Commanding Officer  
Western Division - Code 09PA  
Naval Facilities Engineering Command  
P. O. Box 727  
San Bruno, CA 94066

Commanding Officer  
Western Division - Code 04  
Naval Facilities Engineering Command  
P. O. Box 727  
San Bruno, CA 94066

Commanding Officer  
Western Division - Code 04B  
Naval Facilities Engineering Command  
P. O. Box 727  
San Bruno, CA 94066

Commanding Officer  
Western Division - Code 05  
Naval Facilities Engineering Command  
P. O. Box 727  
San Bruno, CA 94066

Commanding Officer  
Western Division - Code 112  
Naval Facilities Engineering Command  
P. O. Box 727  
San Bruno, CA 94066

Public Works Officer Naval Station Treasure Island San Francisco, CA 94130	Staff Civil Engineer Pearl Harbor Naval Shipyard Box 400 FPO San Francisco 96610	Staff Civil Engineer U.S. Naval Station FPO San Francisco 96651
Asst. Resident OIC of Construction Bldg 506 Hunters Point Naval Shipyard San Francisco, CA 94135	Staff Civil Engineer Naval Supply Center Box 300 FPO San Francisco 96610	Staff Civil Engineer U.S. Naval Station FPO San Francisco 96654
Public Works Officer San Francisco Bay Naval Shipyard Hunters Point Division San Francisco, CA 94135	Commander Pacific Division Naval Facilities Engineering Command FPO San Francisco 96610	Asst. Public Works Officer San Miguel, Naval Communications Station Box 1585 FPO San Francisco 96656
Public Works Department (183) Naval Air Station Alameda, CA 94501	RDT&E Liaison Officer Pacific Division - Code 403 Naval Facilities Engineering Command FPO San Francisco 96610	Public Works Officer U.S. Naval Communication Station FPO San Francisco 96680
Public Works Officer Mare Island Naval Shipyard Vallejo, CA 94592	Mr. T. M. Ishibashi Navy Public Works Center Engineering Department - Code 200 FPO San Francisco 96610	Officer in Charge of Construction Naval Facilities Engineering Command Contracts FPO San Francisco 96680
Asst. Public Works Officer Naval Support Activity Mare Island Naval Shipyard Vallejo, CA 94592	Staff Civil Engineer Naval Supply Center Box 300 FPO San Francisco 96610	U.S. Naval Support Force Antarctica Detachment 1 FPO San Francisco 96690
Public Works Officer Code 70 Naval Supply Center Oakland, CA 94625	Public Works Officer U.S. Naval Air Station FPO San Francisco 96611	Public Works Officer Naval Facility Coos Head Empire Station Coos Bay, OR 97420
Public Works Officer Naval Hospital Oakland, CA 94627	Public Works Officer Engineering Division Naval Ammunition Depot FPO San Francisco 96612	Public Works Officer Naval Support Activity Seattle, WA 98115
Mr. H. Wheeler Code 73.13 Naval Fuel Department Point Molate Richmond, CA 94804	Public Works Officer U. S. Naval Station Box 15 FPO San Francisco 96614	Public Works Officer Naval Air Station Whiley Island Oak Harbor, WA 96277
Public Works Officer Naval Communication Station San Francisco Rough and Ready Island Stockton, CA 95203	Mr. D. K. Moore Hawaii Laboratory Naval Undersea Center FPO San Francisco 96615	Public Works Dept., Code 400 Puget Sound Naval Shipyard Bremerton, WA 98314
Public Works Officer Naval Facility, Centerville Beach Ferndale, CA 95536	Public Works Officer U.S. Marine Corps Air Station FPO San Francisco 96615	Public Works Officer Naval Torpedo Station Keyport, WA 98345
Base Civil Engineer Det 3, 15th ABW (PACAF) APO San Francisco 96305	Staff Civil Engineer U. S. Naval Communication Station FPO San Francisco 96630	Commanding Officer U.S. Navy Public Works Center Box 13 FPO Seattle 98762
Director, Engineering Division Officer in Charge of Construction Naval Facilities Engineering Command Contracts, Southwest Pacific APO San Francisco 96528	Staff Civil Engineer U.S. Naval Station FPO San Francisco 96630	Commanding Officer U. S. Naval Air Facility Box 15 FPO Seattle 98767
Headquarters Kwajalein Missile Range Box 26, Attn: SSCR-RKL-C APO San Francisco 96555	Officer in Charge of Construction Naval Facilities Engineering Command Contracts, Marianas FPO San Francisco 96630	Public Works Officer U.S. Naval Security Group Activity FPO Seattle 98768
Commanding Officer Mobile Construction FOUR FPO San Francisco 96601	Staff Civil Engineer U.S. Naval Station FPO San Francisco 96630	Public Works Officer Fleet Activities FPO Seattle 98770
Commanding Officer Mobile Construction Battalion TEN FPO San Francisco 96601	Technical Library Engineering Department U. S. Navy Public Works Center Box 6 FPO San Francisco 96651	Public Works Officer Marine Corps Air Station (H) FPO Seattle 98772

Public Works Officer  
Marine Corps Base  
Camp Smedley D. Butler  
FPO Seattle 98773

Public Works Officer  
U. S. Naval Station  
FPO Seattle 98791

Public Works Officer  
U.S. Naval Communication Station  
Box 30  
FPO Seattle 98791

Colleges, etc.

Prof. W. E. Heronemus  
Civil Engineering Dept.  
University of Massachusetts  
Amherst, MA 01002

MIT Libraries  
Technical Reports - Room 14 E-210  
Massachusetts Institute of Technology  
Cambridge, MA 02139

Document Library L0-206  
Woods Hole Oceanographic Institution  
Woods Hole, MA 02543

Prof. R. W. Corell  
Mechanical Engineering Dept.  
Kingsbury Hall  
University of New Hampshire  
Durham NH 03824

Reprint Custodian  
Dept. of Nautical Science  
U. S. Merchant Marine Academy  
Kings Point, NY 11024

Mr. R. F. Snyder  
Ordnance Research Laboratory  
Pennsylvania State University  
State College, PA 16801

Professor Adrian F. Richards  
Marine Geotechnical Laboratory  
Lehigh University  
Bethlehem, PA 18015

Dr. Houan Yeh  
Towne School of Civil & Mechanical Eng.  
University of Pennsylvania  
Philadelphia, PA 19104

Mr. T. W. Mermel  
4540 43rd St., NW  
Washington, D.C. 20016

Library of Congress  
Science & Technology Division  
Washington, DC 20540

W. F. Searle, Jr.  
National Academy of Engineering  
808 Timber Branch Parkway  
Alexandria, VA 22302

Public Documents Department  
Wm. R. Perkins Library  
Duke University  
Durham, NC 27706

Dr R. C. Jordan  
Dept of Mechanical Engineering  
University of Minnesota  
Minneapolis, MN 55455

Dr N. M. Newmark  
1114 Civil Engineering Bldg  
University of Illinois  
Urbana, IL 61801

Professor W. J. Hall  
1108 Civil Engineering Bldg  
University of Illinois  
Urbana, IL 61801

Metz Reference Room  
Civil Engineering Dept  
8106 Civil Engineering Bldg  
University of Illinois  
Urbana, IL 61801

Mr. G. A. Sutton  
Planning & Development  
State Highway Commission  
State Office Bldg  
Topeka, KS 66612

Acquisition Dept - Serials Section  
University of Nebraska Libraries  
Lincoln, NE 68508

Robert D. Tent  
Undersea Services Division  
Fluor Ocean Services Inc  
P. O. Drawer 310  
Houma, LA 70360

Department of Oceanography  
Texas A & M University  
College Station, TX 77843

Civil Engineering Dept  
Texas A & M University  
College Station, TX 77843

R. C. Dehart  
Southwest Research Institute  
8500 Culebra Road  
San Antonio, TX 78228

Wang Civil Engineering Research Facility  
P. O. Box 188 - CERF  
University Station  
University of New Mexico  
Albuquerque, NM 87106

Aerospace Corporation  
Acquisitions Group  
P. O. Box 92957  
Los Angeles, CA 90009

TRW Systems  
Attn: P. K. Dai R1/2178  
1 Space Park  
Redondo Beach, CA 90278

Dr F. N. Spiess  
Marine Physical Laboratory  
Of the Scripps Institution of Oceanography  
University of California  
San Diego, CA 92152

Engineering Library  
Stanford University Libraries  
Stanford, CA 94305

Dept of Naval Architecture  
College of Engineering  
University of California  
Berkeley, CA 94720

Engineering Library  
University of California  
Berkeley, CA 94720

Melvin R. Ramey  
Civil Engineering Dept  
University of California, Davis  
Davis, CA 95616

H. Norby Neilsen  
University of Hawaii  
Honolulu, HI 96822



